Conducting barriers for direct contact of PZT thin films on reactive substrates

T. Maeder, P. Muralt, L. Sagalowicz, and N. Setter

Laboratoire de Céramique, Département des Matériaux, Ecole Polytechnique Fédérale de Lausanne (EPFL), CH-1015 Lausanne, Switzerland

Version of record: Journal of the Electrochemical Society 146 (9), 3393-3397, 1999.
http://hdl.handle.net/10.1149/1.1392484

Abstract

Several bottom electrode systems for ferroelectric oxide thin film deposition onto reactive substrates or reactive metal films have been investigated with respect to chemical barrier properties and contact resistivity. Such electrode systems should not deteriorate by oxidation, and should prevent oxygen diffusion into the underlying base metal**.** First, the protective performance of Pt, Ru, RuO_2 / Ru and Cr has been evaluated on reactive substances such as W, Zr, Mo and TiN. On most materials, a reactive and passivating metal such as Cr offers protection up to a higher temperature than noble metals. This is explained by preferential oxidation. On Cr, a RuO_2 electrode allowed oxidation resistance to more than 800°C without any Cr diffusion: the RuO_2 serves both as an electrode and as a barrier to Cr. In order to reduce the contact resistance due to the formation of a Cr_2O_3 film at the RuO_2 / Cr interface, a Ru interlayer was inserted, giving a RuO_2 / Ru / Cr. This combination allowed to maintain a low contact resistance up to 700°C.

Introduction

Recently, thin films of $Pb(Zr,Ti)O_3$ (PZT) and other oxide ferroelectrics have attracted considerable attention due to their possible application in memories and miniature sensors and actuators [1]. However, severe integration problems are encountered in many cases, since PZT thin films need to be grown at rather high deposition temperatures (550 to 700°C) in an oxidizing atmosphere. Deterioration of properties or even delamination may result from interdiffusion and oxidation. The problem is usually solved by adding a chemically very stable oxide (as, e.g. SiO_2) or nitride (as e.g. Si_3N_4) barrier layer between a reactive substrate like silicon, and the bottom electrode (usually Pt/Ti or Ta) on which the PZT is grown. This procedure is not always satisfying, because these barrier layers are electrical insulators. For high density FRAM's a direct electrical contact between drain and bottom electrode are needed [2]. In ultrasonic applications, where high ac currents are flowing through the bottom electrode, a well conductive, i.e., a few micrometer thick electrode of another material than the expensive platinum would be desirable [3]. In the latter case it might be advantageous to take a metal foil as substrate, which than could carry the ac current.

In what follows the reactive substance below the electrode system is called base metal, be it a substrate like a metal foil, silicon, etc., or be it a metal layer such as a tungsten or nickel etc. serving as a conductor on a arbitrary substrate. Due to extensive oxidation and diffusion,

direct deposition of PZT on common metals such as Cr, Zr and Ni is not possible [4]. With a Pt / Ti / Si sequence, extensive out-diffusion of Ti and Si takes place during $SrTiO_3$ capacitor film growth [5]. Replacing Ti with Ta reduces diffusion, but leads to very high contact resistance, presumably due to oxidation of the Ta to Ta_2O_5. Dhote et al. [6] replaced Ti with TiN (Pt/TiN/Si), allowing deposition of LSCO / PZT / LSCO stacks up to 550°C. However, this solution is limited to that temperature, above which TiN oxidizes rapidly [7]. Dormans et al. [2] used a Pt / RuPt alloy / Ti / W plug on silicon that allowed PZT deposition up to 700°C without detectable contact resistance. In a previous paper [8], we demonstrated PZT deposition at 570°C on a very reactive metal (Zr), using a RuO_2 / Cr metal combination (Fig. 1). The same bilayer was found to work on Si [9] using an additional TiN or TiW barrier layer between Si and Cr.

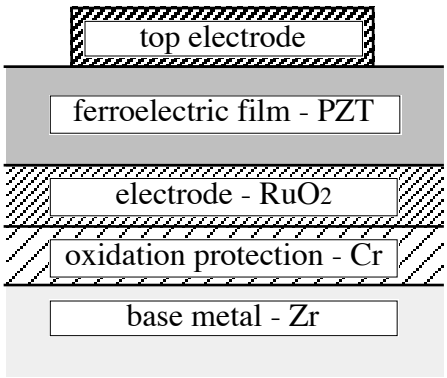

Figure 1. Example electrode system for deposition of PZT onto Zr [8].

Our earlier work showed that Cr does not diffuse through RuO_2 and protects well against oxygen diffusion by oxide scale formation. As chemical barrier, electrode layers containing a Cr thin film are far superior to Pt, Ru and RuO_2 / Ru electrodes. However, contact resistance could be high and dependent on the thermal budget, due to formation of a Cr_2O_3 layer between Cr and RuO_2. In this work, we (i) extend the study of the protective effect of Cr to other reactive substances (W, Zr, Mo and TiN), in order to have a general understanding of protection and (ii) we examine the effect of introducing a Ru interlayer between RuO_2 and Cr (giving the RuO_2 / Ru / Cr sequence) in order to lower the contact resistance. We expect Cr will oxidize first in the grain boundaries of the Ru, retarding the formation of a continuous Cr_2O_3 layer.

Experimental

All samples were deposited as film sequences onto SiO_2 (1 μm) / Si substrates, using a Nordiko 2000 sputtering system. The metal / electrode sequences were put down at 500°C, in order to ensure dense, high quality films. Thin (10 to 20 nm) Ti adhesion layers, given in parentheses (Ti) in Table I, were used where delamination problems were encountered or expected.

The oxidation resistance of each layer sequence, composed of an electrode on a base metal (Zr, W, Mo, TiN) as defined in Table I, was tested by means of heat treatments in an oxygen ambient. Each sample was subjected to cumulative 10 min oxidation periods at 200, 300,

400, 450, then every 50°C up to 800°C, in a lamp furnace and in a pure oxygen stream at atmospheric pressure. After each oxidation period, the samples were cooled to room temperature for ex situ electrical and thickness measurements (see below). Alternatively, to assess the effect of thermal cycling up to 700°C, a second set of samples was subjected to a single oxidation run having a thermal budget roughly equivalent to that of the cycled specimens, as shown in Fig. 2.

Global degradation of the samples due to oxidation was assessed by measuring the effect of oxidation treatments on the electrical resistance of a strip of film (typically 3-5 mm wide, see Fig. 3a). This method is similar to that used by Cvelbar et al. [11], except that all our measurements were carried out *ex-situ* at room temperature in between oxidation tests. Additionally, the thickness of each stack was measured using an Alpha-Step profilometer. Thus test indicates the degree of degradation due to the volume increase brought about by oxidation. Table I lists the samples tested for oxidation resistance. These may be divided into three categories

1. Individual layers (reference)
2. Protection against oxidation by Cr or noble metals
3. RuO_2 electrode on Cr or Ru/Cr, as a complement to contact resistance measurements.

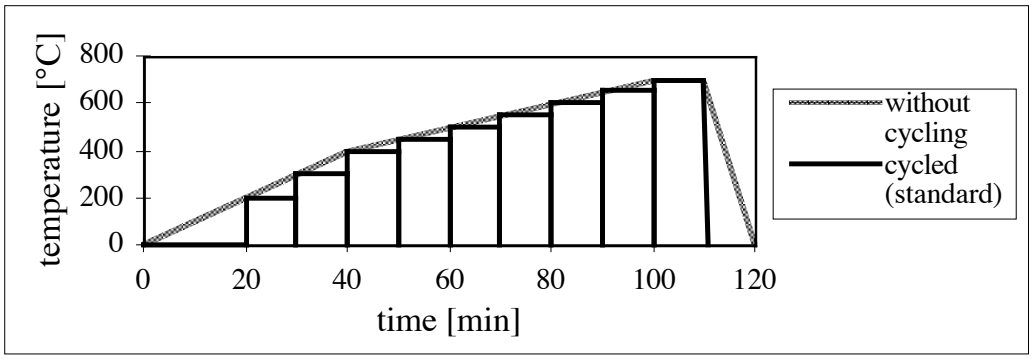

Figure 2. Comparison of the 2 oxidation treatments at 700°C. The rise and fall times for the cycled samples (1 min) are not shown.

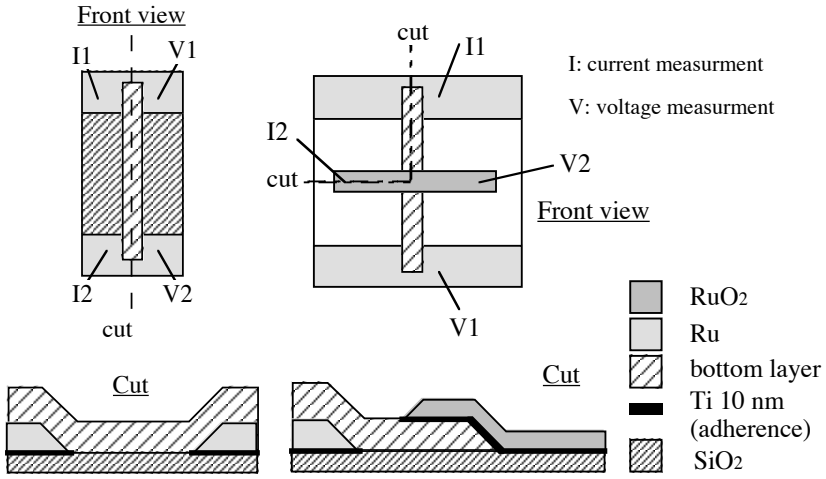

(a) (b)

Figure 3. Samples for measurement of electrical resistance along the film (a) and contact resistance (b).

Stack (Ti): thin Ti adhesion layer	**Individual layer thicknesses** (estimated) [nm]	**Total thickness** (measured) [nm]
Individual films (references)		
Zr	1342	1342
W / (Ti)	398 / 13	411
Mo / (Ti)	876 / 20	896
TiN / (Ti)	517 / 13	530
Protection with Cr alone		
Cr / Zr	270 / 1355	1625
Cr / (Ti) / W / (Ti)	270 / 13 / 642 / 20	945
Cr / (Ti) / W / (Ti)	500 / 13 / 522 / 20	1055
Cr / (Ti) / Mo / (Ti)	490 / 13 / 900 / 20	1423
Cr / (Ti) / TiN / (Ti)	490 / 13 / 134 / 13	650
Protection with Pt, Ru, RuO_2 / Ru		
Ru / Zr	150 / 1373	1523
Pt / (Ti) / W / (Ti)	250 / 13 / 543 / 20	826
Ru / (Ti) / W / (Ti)	250 / 13 / 547 / 20	830
RuO_2 / Ru / (Ti) / W / (Ti)	300 / 150 / 13 / 434 / 13	910
RuO_2 electrode on Cr or Ru / Cr		
RuO_2 / (Ti) / Cr / (Ti)	340 / 28 / 500 / 13	881
RuO_2 / Ru / Cr / (Ti)	290 / 150 / 447 / 13	900

Table I. List of samples for characterization of global oxidation resistance.

Sequences **(top x bottom leg)**	**Thicknesses [nm]**
RuO_2 / (Ti) × Ru / Cr / (Ti)	300 / (10) × 150 / 430 / (10)
RuO_2 / (Ti) × Cr / (Ti)	300 / (10) × 500 / (10)

Table II. Samples for contact resistance measurements.

For contact resistance measurements, two strips (the top and bottom film) are deposited perpendicular to each other forming a cross (Fig. 3b). This allows evaluation of the contact resistance by a four-wire method, eliminating the effect of the electrical resistance of the cross legs. Moreover, we used finite difference calculations to compensate the error due to an inhomogeneous voltage distribution inside the contact area when contact resistance is small. Table II lists these samples, which both have corresponding analogues in Table I.

Finally, selected samples were examined by transmission electron microscopy (TEM).

Results

Reactive metals and TiN alone

The relative conductance (conductance of the sample after relative to as-deposited) as a function of cumulative oxidation temperature is given in Fig. 4 for the reactive films (Zr, Mo, W and TiN), with and without a Cr protective layer. All of the unprotected layers oxidize extensively at quite low temperatures, as evidenced from the rapid loss of electrical conductivity. Similar results were obtained for other reactive substances such as Ti, Nb and Ta. These substances definitely need protection against oxidation for the 550-700°C PZT deposition temperature range.

Oxidation resistance of stacks protected with Cr

As evidenced from Fig. 4, a Cr overlayer clearly has a protective behavior on all substances. However, this protection is limited to about 600°C in the case of Zr. Above 650°C, the structure delaminates. On the other hand, Cr is very effective at protecting all the other films at least up to 800°C, forming a layer of Cr_2O_3 on the sample surface. While conductivity does eventually drop by oxidation and eventually alloying (the increases of conductance in the 550-700°C range is attributed to annealing of Cr), no delamination is observed. Also, in these instances, the corresponding thickness increases (Fig. 5) agree roughly with that of the single Cr film and the results of other oxidation studies on Cr [12]. This confirms the protective effect; the degradation is governed mainly by the oxidation of Cr. The small observed differences can be ascribed to (i) slight temperature inhomogeneities in our lamp furnace, (ii) measurement errors (±40 nm), (iii) influence of growth kinetics of the Cr_2O_3 scale by small W, Mo or Ti additions and (iv) influence of the underlayer on the Cr film properties (density, etc.).

From our earlier studies [8,13], we expected good protective behavior due to the reactivity of Cr and the formation of a dense, protective scale of Cr_2O_3. Obviously, this does not work fully in the case of Zr. As compared to the oxidation of unprotected Zr, the oxidation below the Cr layer is slowed down, but is not stopped.

Oxidation resistance of stacks protected with Pt, Ru and RuO_2 / Ru

The relative conductance results are given in Fig. 6 for this second set of stacks. Unlike Cr, these nobler compounds showed limited protective behaviour in all circumstances, with failure temperatures in the 600-700°C range. Additional tests of Pt on Ti, Zr, Nb, Ta, TiN and ZrN, which were carried out in less detail, also showed similar failure temperatures. On W, the failure temperatures are somewhat lower (100°C) than that of the very similar Pt / RuPt alloy / Ti stack used by Dormans et al. [2].

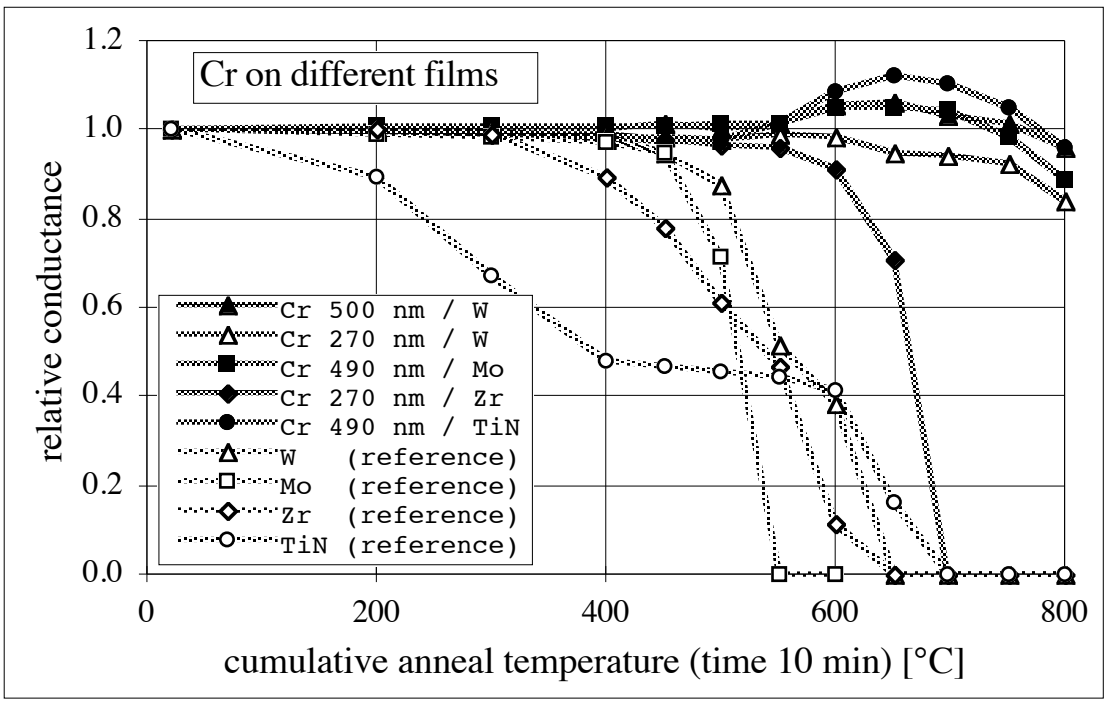

Figure 4. Relative conductance as a function of cumulative oxidation temperature of Cr-protected films. Unprotected versions are given as a reference.

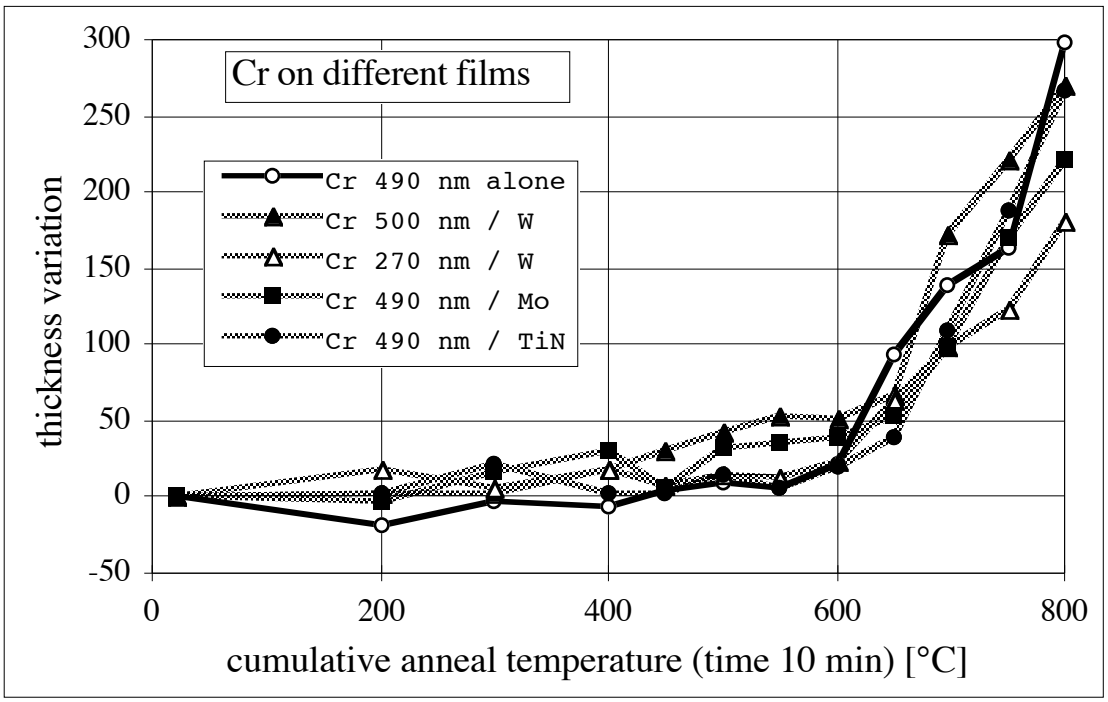

Figure 5. Thickness increase as a function of cumulative oxidation temperature of Cr-protected samples (except Zr). Cr alone deposited in the same conditions is given as a reference.

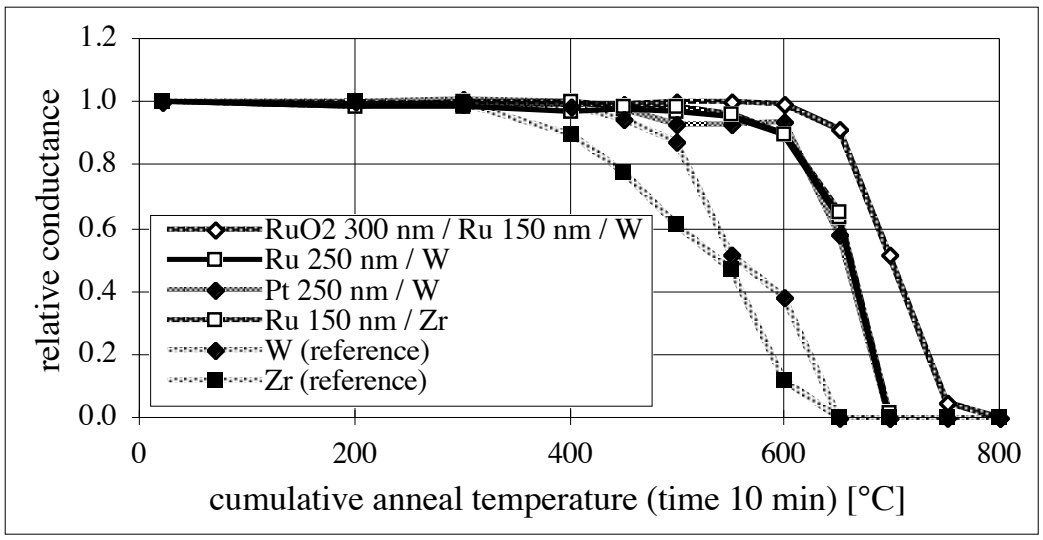

Figure 6. Relative conductance as a function of cumulative oxidation temperature of films protected by Ru, RuO_2/Ru or Pt. Unprotected versions are given as a reference.

Effect of stresses due to thermal cycling on oxidation resistance

The effect of thermal cycling was assessed by comparing the results obtained on samples subjected to cumulative oxidation runs up to 700°C (cycled) to those obtained from samples subjected to a single oxidation run having a similar thermal budget (Fig. 2). The results are given in Table III. While no significant change is observed for samples which clearly failed below 700°C (Ru / Zr, Pt / W) or withstood higher temperatures (Cr / W), some "borderline" samples such as Cr / Zr, Ru / W and RuO_2 / Ru /W do perform significantly better, indicating the stresses due to thermal cycling can contribute significantly to degradation.

Stack	Relative conductance Cycled to 700°C	Relative conductance Single run to 700°C	Thickness increase Cycled to 700°C [nm]	Thickness increase Single run to 700°C [nm]
Cr 270 nm / Zr	x	0.15	x	880
Ru 150 nm / Zr	x	x	x	x
Cr 270 nm / W	0.94	0.96	100	110
Pt 250 nm / W	x	x	x	x
Ru 250 nm / W	x	0.65	x	1640
RuO_2 / Ru / W	0.52	0.97	30	90

Table III. Effect of thermal cycling on various samples. The measurement error on thickness variation is about ±40 nm. (x = delamination).

Contact resistance of RuO_2 × Cr and RuO_2 × Ru / Cr

The contact resistance of the two samples listed in Table II are shown in Fig. 7. Both samples do not delaminate or structurally fail in any way up to 800°C. RuO_2 x Cr already has a significant contact resistance in the as-deposited state. As the sample starts to react (450-650°C), the resistance drops, than increases again beyond this range to very high values. Simpler behavior is observed when a Ru layer is inserted: the sample keeps a low contact resistance up to 700°C, above which an increase is observed. Adding a Ru layer therefore tends to suppress the initial contact resistance and also shifts the temperature above which an insulating layer forms by 50°C.

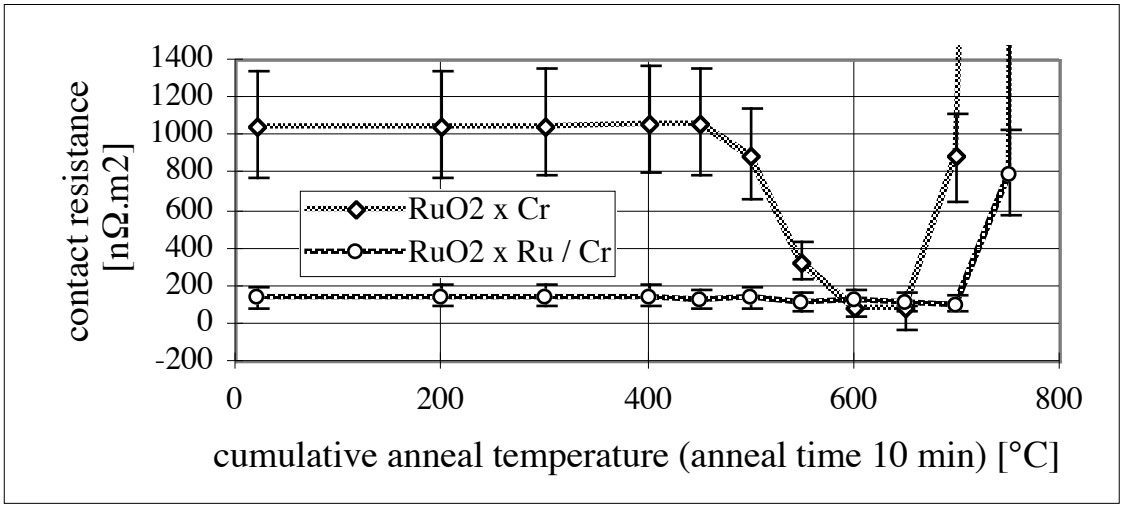

Figure 7. Evolution of contact resistance as a function of cumulative oxidation temperature.

In-plane conductivity of RuO_2 / Cr and RuO_2 / Ru / Cr

The relative and square conductances as a function of cumulative oxidation temperature are given in Fig. 8 for the in-plane analogues to the contact resistance measurement samples. The effect of annealing, followed by oxidation of Cr can be seen on the curves of Cr and RuO_2 / Cr (hump in the 600-800°C range) in the upper part of Fig. 8. Since the three 3 stacks have been deposited using the same individual layer thicknesses and deposition conditions, comparison of the absolute conductance values allows one to discriminate the contributions from the different layers (bottom part of Fig. 8). Neglecting any interaction between the layers, the first and the succeeding two interval curves show a rough estimate of the contribution of Cr, RuO_2 and Ru, respectively. For example, the contribution of the Ru layer can be estimated by subtracting the square conductance of Ru/Cr from the one of RuO_2/Ru/Cr. In this view, one can see that the Ru contribution is abruptly reduced around 600°C, even though the Ru layer is still present (see TEM below). On the other hand, the RuO_2 contribution seems pretty much unchanged.

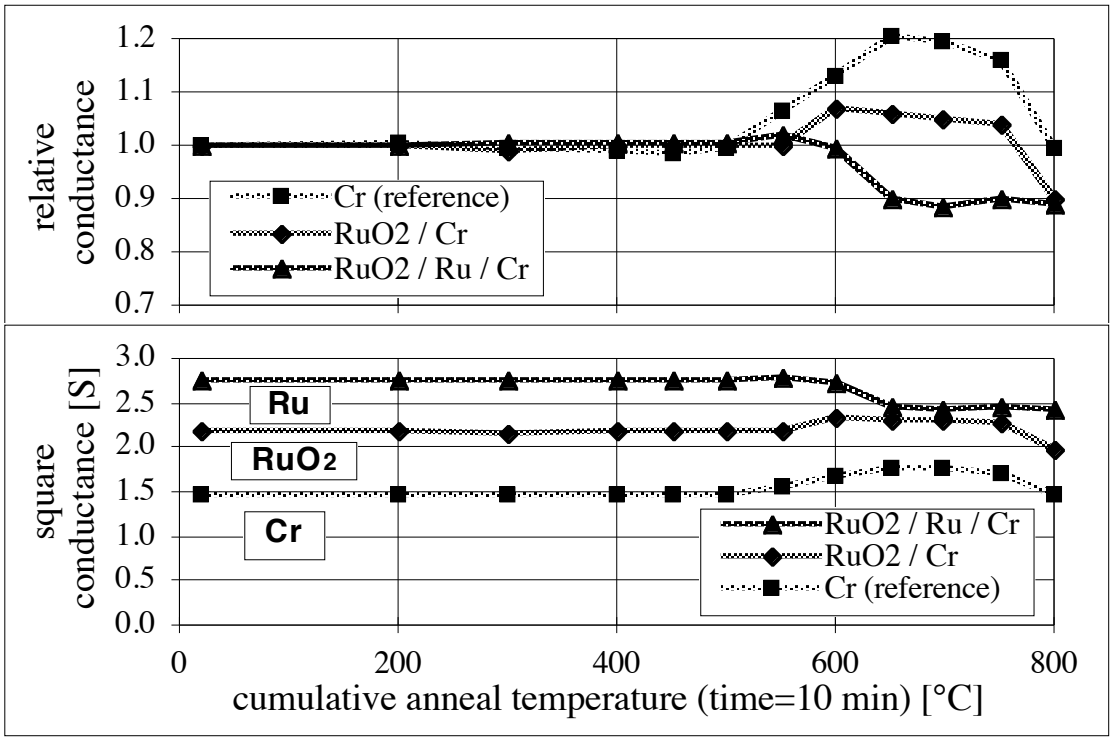

Figure 8. Relative conductance and square conductance as a function of cumulative oxidation temperature of RuO_2 / Cr and RuO_2 / Ru / Cr, with Cr alone as a reference. In the square conductance view, the three labeled intervals approximately represent the respective individual contributions to the stack conductance, and the results for RuO_2 / Ru / Cr are multiplied by 1.1 to compensate for correspondingly thinner Cr and RuO_2 layers.

TEM observations of RuO_2 / Ru / Cr

A cross-section of the RuO_2 / Ru / Cr interfaces was observed by TEM after the tests (all anneals up to 800°C), and compared to the corresponding cross-section of RuO_2 / Cr, as shown in Fig. 9. In both cases, a thick layer of Cr_2O_3 has formed at the RuO_2 / Cr interface and no Cr_2O_3 is detected at the top of the RuO_2. The presence of Cr_2O_3 was confirmed by electron diffraction and electron energy loss spectroscopy (EELS).

Since Cr is much more reactive with oxygen than Ru [14], Ru essentially plays the role of an inert metal marker for Cr and oxygen diffusion - as Cr will oxidize preferentially. Cr_2O_3 has formed below, inside and above Ru, with about twice more above Ru than below it, justifying *a posteriori* the choice of the RuO_2 × Ru / Cr configuration instead of RuO_2 / Ru × Cr. From the Cr_2O_3 distribution, we find the growth of the Cr_2O_3 scale occurs through both Cr and oxygen diffusion, in agreement with published results on oxidation of bulk alloys [15,16], with a larger Cr contribution.

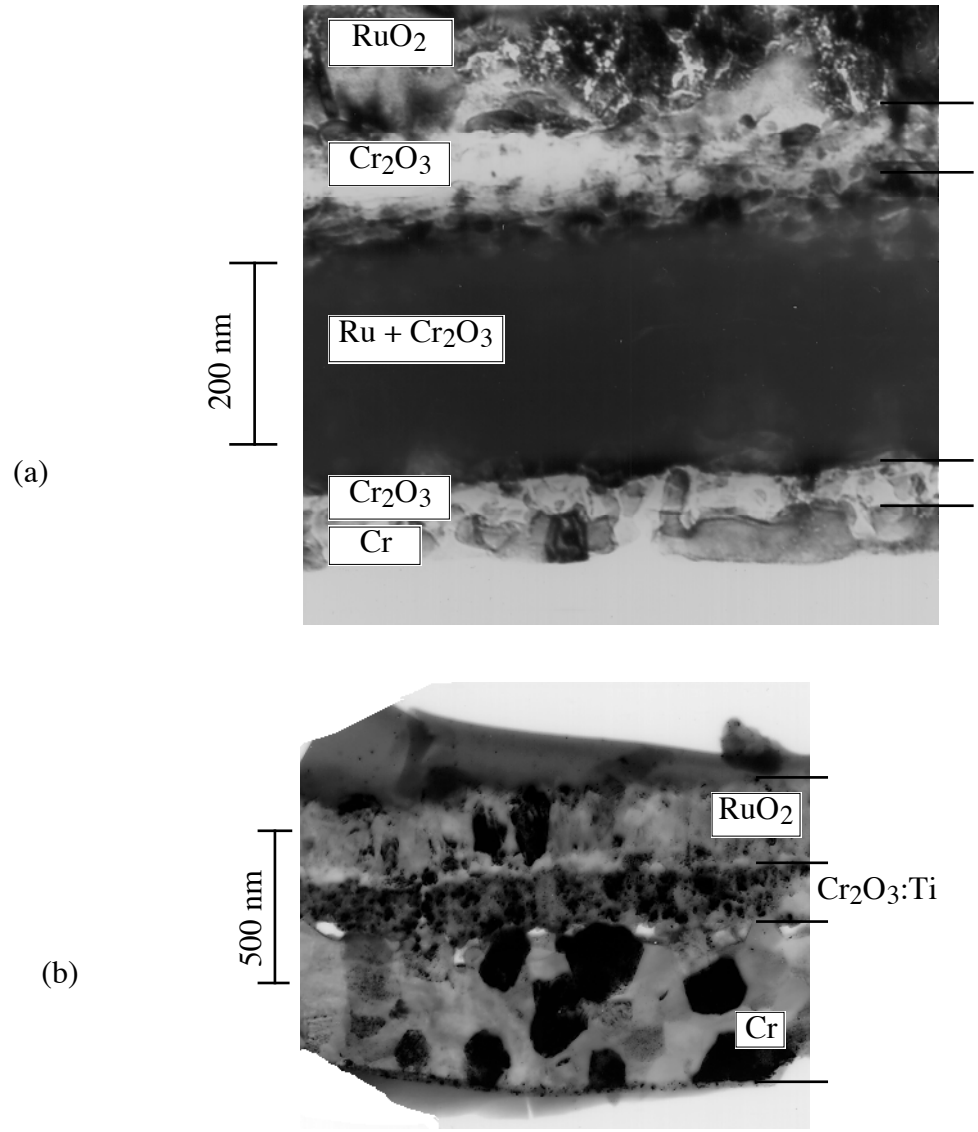

Figure 9. TEM cross-section after heat-treatment in oxygen at 800°C: (a) bright-field image of RuO_2 / Ru / Cr, (b) dark-field image of RuO_2 / Cr. Note the difference in scale.

Discussions

Performance and limitations of the oxidation barriers

At high temperatures, interdiffusion is likely to occur between the protective metal layer (Cr or noble metals) and the reactive material it protects. As a consequence, the stack surface will effectively become an alloy, and the preferred oxide formed will usually be the stabler one (selective oxidation) [17]. Hence, if Cr is more reactive than the underlying metal, a protective Cr_2O_3 scale will form. Conversely, an underlayer more reactive than Cr and whose oxide is not protective (such as Zr) will catastrophically oxidize above a certain temperature. Comparing oxidation free energies per mole of oxygen [14], we can predict, in the case the underlying layer has reached the film surface:

1. Cr will not protect Zr, as Zr is more reactive than Cr.
2. Cr will protect W, Mo and TiN.
3. Ru and Pt will protect none of the abovementioned reactive substances.

These predictions are in very good agreement with our results. While one would expect a bigger difference between Ru and Cr on Zr because of the considerable difference in oxygen reactivity, this effect may be counterbalanced by greater diffusivity between Cr and Zr. While both the Ru-Zr and Cr-Zr systems show extended miscibility [18], Cr has a lower melting point than Ru (1857° vs. 2310°C [14]).

As to TiN, its reactivity with oxygen is smaller than that of Cr (contrarily to Ti, which exhibits a higher reactivity). Also, diffusion of TiN through Cr is unlikely up to very high temperatures. These features of TiN can thus be exploited to separate Cr from highly reactive materials such as silicon, which readily forms a silicide with Cr at ferroelectric film processing temperatures [9,19]. In this way, a separation of the two barrier problems, oxygen diffusion on one hand and reactive metal diffusion on the other, can be separated. The other oxidation mechanism (diffusion of oxygen through the Cr) is bound to be very slow through a dense film because the high reactivity of Cr imposes a very low maximum activity of oxygen: the activity calculated from thermodynamic data [14] is in the 10^{-27} Pa range at 700°C.

On the other hand, oxygen diffusion through noble metals is likely to occur because of the corresponding high equilibrium metal-oxide activities. Therefore, a noble metal barrier may fail both by (i) out-diffusion and selective oxidation of the underlying metal and (ii) by in-diffusion of oxygen. These phenomena are basically the same as those occurring in bulk alloys: selective oxidation at the surface (scale formation) or in the sample (internal oxidation) [17].

Fig. 8a is a direct confirmation of the bad barrier characteristics of noble metals. As Cr_2O_3 is found both below and above Ru, one can conclude that Ru is neither a good barrier against oxygen, nor against Cr diffusion. This might be generalized to any noble metal / reactive metal stack: in a recent paper [20], we show the oxidation behavior of Ti, Zr and Ta adhesion layers for Pt metallizations (whether the adhesion layer oxidizes in and above the Pt or below it) is determined by the respective cation and oxygen mobilities in the corresponding oxide.

Finally, one should note that pure Cr was chosen rather than an alloy for simplicity in this study. In practice, Cr_2O_3-forming alloys may show a better oxidation resistance [Whittle 19]. Our preliminary results on stainless steel films also show much better resistance to oxidation than pure Cr films.

Contact resistance

Without a Ru layer, the evolution of the RuO_2 / (Ti) / Cr contact resistance can be separated into three separate steps :

1) oxidation of the Cr surface and Ti adhesion layer by the reactive plasma used during RuO_2 deposition, giving a relatively resistive interface,
2) lowering of the contact resistance in the 400-600°C temperature range by oxidoreduction or intermixing of Cr_2O_3, TiO_2 and RuO_2 without diffusion of atmospheric oxygen through the RuO_2, and
3) formation of a thick, insulating layer of Cr_2O_3 at higher temperatures, where RuO_2 is no longer a barrier against oxygen diffusion.

The insertion of a Ru layer, by avoiding contact between Cr and RuO_2, suppresses the initial contact resistance (1) and hence step 2, and retards step 3 by about 50°C. The reason for this latter result is evident from the TEM pictures, although they were taken above the temperatures at which this mechanism is effective: initially, Cr_2O_3 forms in the Ru grain boundaries, and this does not give rise to contact resistance as long as the Cr_2O_3 has not extended to a continuous layer between RuO_2 and Ru or Ru and Cr, which, from the contact resistance measurements, happens between 700 and 750°C.

Indirect confirmation of prior Cr_2O_3 formation in Ru is given by the in-plane resistance measurements (Fig. 8), which show that the Ru contribution to in-plane conductance diminishes around 600°C. Obviously, an insulating layer must have formed between the Ru columnar grains (the in-plane conductance of Ru is lowered) but not above or below (the contact resistance does not increase).

Up to 700°C, the measured contact resistance is low enough for piezoelectric devices. However, for memory applications, more sensitive measurement techniques and layouts are needed in order to judge the performance of this barrier type. Compared to the version without Ru, this new barrier structure does not depend on a particular heat treatment to lower the contact resistance, removing the necessity of a special annealing treatment. Also the Ru and Cr based thin films are more easily plasma etched than the platinum based electrodes and therefore should be compatible with high density integration.

Conclusions

We have shown that the protection of reactive layers, needed for successful deposition of oxide ferroelectric films onto reactive substrates such as metals or Si, obeys the same basic rules as the oxidation behavior of bulk alloys. Namely, a sufficiently reactive element, such as Cr, is needed. When this element is more reactive than the layer it protects, outstanding protection is obtained, as in the case of Cr on W, Mo and TiN, where protection is maintained up to at least 800°C. However, when Cr is deposited on an even more reactive element such as Zr, protection is limited by interdiffusion between the metals, followed by selective oxidation of Zr.

Hence, noble metals always have limited effectiveness as barriers, and oxidation of the underlying reactive layer will occur by in-diffusion of oxygen or out-diffusion of the metal, depending on the diffusion characteristics of the formed oxide.

RuO_2 is a good electrode for PZT on Cr, as it prevents Pb and Cr diffusion. However, the trapping of Cr underneath the RuO_2 favors the formation of a continuous Cr_2O_3 layer, possibly giving rise to a high contact resistance. Insertion of a Ru layer between RuO_2 and Cr alleviates this problem, giving a well conducting RuO_2 / Ru / Cr barrier scheme, which shows low contact resistance up to above 700°C. The Ru layer effectively "short-circuits" the Cr_2O_3, which forms first as a discontinuous film in the Ru grain boundaries. Moreover, the initial contact resistance due to oxidation of the Cr during RuO_2 deposition is suppressed. The contact resistance of this barrier is low enough for high-frequency piezoelectric and possibly for memory applications.

Acknowledgements

This work has been funded the Swiss priority program for materials research (PPM). The microscopy work was done at the CIME at the EPFL.

École Polytechnique Fédérale de Lausanne assisted in meeting the publication costs of this article.

References

1 S.B. Krupanidhi, “Ferroelectric thin films and device applications”, dans “NATO ASI proceedings” 234, Bad Windsheim, Kluwer, Dordrecht, RFA (1992).

2 G.J.M. Dormans, J.H.H.M. Kemperman, R.A.M. Wolters, P.J.v. Veldhoven, M. de Kejser, R.B.F. Janssen, M.J.E. Uleaners et P.K. Larsen, “Direct-contact ferroelectric capacitors for memory applications”, Microelectronic Engineering **29**, pp 33-36 (1995).

3 M.-A. Dubois, P. Muralt, "PZT thin film actuated elastic fin micromotor", IEEE Transactions on Ultrasonics, Ferroelectrics and Frequency Control **45** (5), 1169-1177, 1998.

4 S.A. Myers et E.R. Myers, “Effect of electrode materials on the microstructure of sol-gel derived PZT ferroelectric thin films”, dans “Materials Research Symposium Proceedings” **243**, pp 107-112, MRS, Pittsburgh (1992).

5 K. Takemura, T. Sakuma, S. Matsubara, S. Yamamichi et H. Yamaguchi, “Barrier mechanism of Pt/Ta and Pt/Ti layers for $SrTiO_3$ thin film capacitors on Si”, Integrated Ferroelectrics **4 (IV)**, pp 305-313 (1994).

6 M. Kohli, C. Wüthrich, K. Brooks, B. Willing, M. Forster, P. Muralt, N. Setter, and P. Ryser, Sensors & Actuators A, 60, 147 (1997).[1]

7 O. Knotek, W.D. Münz et T. Leyendecker, “Industrial deposition of binary, ternary, and quaternary nitrides of titanium, zirconium and aluminium”, Journal of Vacuum Science and Technology A **5** (4), pp 2173-2179 (1987).

8. T. Maeder, P. Muralt, L. Sagalowicz, I. Reaney, M. Kohli, A. Kholkin et N. Setter, “$Pb(Zr,Ti)O_3$ thin films on zirconium membranes for micromechanical applications”, Applied Physics Letters **68** (6), pp 776-778 (1996).

9 T. Maeder, L. Sagalowicz et P. Muralt, “Buffer electrodes for deposition of lead zirconium titanate films on metallic substrates”, dans “Proceedings of the 6th European Conference on Applied Surface and Interface Analysis ECASIA’95”, Montreux, pp 931-934, Wiley & Sons (1995).

10 T. Maeder, P. Muralt and L. Sagalowicz, "Growth of (111)-oriented PZT on RuO_2(100)/Pt(111) electrodes by in-situ sputtering", Thin Solid Films 338 (2), 1-7, 1999.[2]

11 A. Cvelbar, P. Panjan, B. Navinsek, A. Zalar, M. Budnar et L. Trontelj, “A continuous electrical resistivity measurement in thin films”, Thin Solid Films **270** (1-2), pp 367-370 (1995).

12 S. Beauvais-Réveillon, A.M. Huntz, G. Moulin et J.J. Bléchet, “Comparison of classical oxidation and laser oxidation of a chromium PVD coating on a pure-iron substrate”, Oxidation of Metals **43** (3-4), pp 279-300 (1995).

13 H.E. Brown, "Lead oxide", International Lead Zinc Research Organization Inc., New York (1985).[3]

---

1 **Erratum**. Correct reference is: A.M. Dhote, S. Madhukar W. Wei, T. Venkatesan, R. Ramesh C.M. Cotell, "Direct integration of ferroelectric La-Sr-Co-O/Pb-Nb-Zr-Ti-O/La-Sr-Co-O capacitors on silicon with conducting barrier layers", Applied Physics Letters 68 (10), 1350-1352, 1996.

2 Exact reference not available at time of print in version of record.

3 **Erratum**. Correct reference is: T. Maeder, P. Muralt, L. Sagalowicz, N. Setter, "Conducting barrier electrodes for direct contact of PZT thin films on tungsten", Journal of the Korean Physical Society 32, S1569-S1572, 1998.

14 R.C. Weast (ed.), “Handbook of Chemistry and Physics”, 64th, CRC Press, Boca Raton, Florida (1984).

15 P. Kofstad, “Defects and transport properties of metal oxides”, Oxidation of Metals **44** (1-2), pp 3-27 (1995).

16 S.C. Tsai, A.M. Huntz et C. Dolin, “Diffusion of O-18 in massive Cr_2O_3 and in Cr_2O_3 scales at 900-degrees-C and its relation to the oxidation-kinetics of chromia forming alloys”, Oxidation of Metals **43** (5-6), pp 581-596 (1995).

17 U.R. Evans, “The corrosion and oxidation of metals: scientific principles and practical applications”, Edward Arnold, London (1960).

18 W.G. Moffatt (ed.), “The Handbook of Binary Phase Diagrams”, **1-2**, General Electric, Schenectady, N.Y., USA (1976-82).

19 F. Mohammadi, “Silicides for interconnection technology”, Solid State Technology (1), pp 65-72 (1981).

20 T. Maeder, L. Sagalowicz et P. Muralt, “Stabilized platinum electrodes for ferroelectric film deposition using Ti, Ta and Zr adhesion layers”, Japanese Journal of Applied Physics **37** (4A), pp 2007-2012.

21 G.C. Whittle et D.P. Wood, “Chromium oxide scale growth on iron-chromium alloys - II. Influence of alloy composition”, Journal of the Electrochemical Society **115** (2), pp 133-142 (1968)